ORIGINAL RESEARCH

Absence of AIF1L contributes to cell migration and a poor prognosis of breast cancer

Peipei Liu[1]
Wenhui Li[2]
Yuanyuan Hu[1]
Youhong Jiang[1]

[1]Molecular Oncology Laboratory of Cancer Research Institute, The First Hospital of China Medical University, Shenyang, People's Republic of China; [2]Gastrointestinal Onco-Pathology Laboratory of Cancer Institute, The First Hospital of China Medical University, Shenyang 110001, People's Republic of China

Correspondence: Youhong Jiang
Molecular Oncology Laboratory of Cancer Research Institute, The First Hospital of China Medical University, No 155, Nanjingbei Street, Heping District, Shenyang 110001, People's Republic of China
Tel +86 24 8328 2315
Email jiangyouhong2000@aliyun.com

Background: Breast cancer is the most common fatal cancer in women worldwide. Previous studies have demonstrated that allograft inflammatory factor 1 like (AIF1L) plays a key role in mammary tumorigenesis, although the mechanism involved remains unclear.

Purpose: The purpose of this study was to assess the clinicopathological and prognostic significance of AIF1L expression levels and biological function in breast cancer.

Patients and methods: We used immunohistochemistry to detect the expression of AIF1L in breast cancer. We also analyzed the expression of AIF1L in breast cancer using the Cancer Genome Atlas (TCGA) cohort and the Cancer Cell Line Encyclopedia (CCLE). Furthermore, both in vitro assays were used to determine the effect of AIF1L on malignant behavior in breast cancer cells.

Results: We detected AIF1L expression in tissue microarrays through immunohistochemistry and found that protein expression was significantly lower in BC tissues (28.6%, 82/287) compared to tumor-adjacent tissues (58.3%, 28/48) (P=0.007). Kaplan-Meier survival analysis revealed that disease-specific survival in BC patients with low AIF1L protein expression was significantly poorer compared to normal controls (P=0.040). In the TCGA cohort, the *AIF1L* gene was downregulated and hypermethylated in tumor samples compared to normal controls. Bioinformatics analysis using CCLE predicted potential biological functions of AIF1L related to tight junctions, cell junctions and focal adhesion. Ectopic expression of AIF1L suppressed MDA-MB-231 migration and invasion. Further evidence confirmed that AIF1L overexpression suppressed cell spreading, altered cell shape and decreased protrusion formation, which was correlated with decreased focal adhesion kinase (FAK) and RhoA expression.

Conclusion: These findings suggest that AIF1L is a potential prognostic biomarker that plays a vital role in regulating the cytoskeleton in breast cancer.

Keywords: AIF1L, breast cancer, cytoskeleton, TCGA

Introduction

Breast cancer (BC) is the leading cause of cancer deaths among females worldwide, with an estimated >500,000 deaths occurring in 2012.[1] As the incidence of BC is increasing rapidly,[2] understanding the biological mechanisms involved and exploring novel targets are urgently needed.

EF-hand proteins are a large number of $Ca2^+$-binding proteins.[3,4] The EF-hand is a helix–loop–helix calcium-binding motif. They are involved in various biological processes, including inflammation, exocytosis, motility, apoptosis, tumor progression, and so on.[3]

Allograft inflammatory factor 1 like (AIF1L) is a protein with EF-hand motifs lacking bound Ca^{2+}.[5] AIF1L consists of 150 amino acids, and the sequence identity to AIF1 is 60%. AIF1 protein is majorly expressed in the immune cells and participates in the inflammatory response and regulation.[6] AIF1 can activate the monocyte/macrophage, microglia, and lymphocyte immune cells, promote the expression of

inflammatory mediators such as cytokines, chemokines, nitric oxide synthase, and boost immune cell proliferation and migration.[7–9] However, AIF1L is majorly expressed in the epithelial cells, such as renal glomerulus and renal tubules, endometrial gland, mammary ductal epithelial cells, glandular epithelium of epididymis, and vascular endothelial cells of spleen.[10,11] Although AIF1 and AIF1L have remarkable sequence homology and structural similarity, they show a distinct pattern of tissue specific expression, so we speculated they have different biological functions.

AIF1L co-localizes with and crosslinks filamentous actin (F-actin) with subcortical filaments and localizes to membrane ruffle-like cellular projections and adhesion structures in a Shigella invasion model.[5] AIF1L deficiency, which was functionally analyzed by siRNA silencing, was shown to result in significant loss and rearrangement of F-actin stress fibers, as shown by phalloidin staining, and led to cytoskeletal injury in immortalized human podocytes.[12] So far, the potential roles of AIF1L in carcinogenesis have not been well characterized.

We studied AIF1L expression levels in BC, the effects of AIF1L on migration and invasion of BC cells, and characterized an AIF1L-related signaling pathway that influences cytoskeletal modifications.

Patients and methods
Cell culture and engineering
The MDA-MB-231 BC cell line was purchased from American Type Culture Collection. Cells were cultured in L15 medium (Hyclone) supplemented with 10% fetal bovine serum (Thermo Fisher Scientific, MA USA). Adenoviruses purchased from Hanbio Biotechnology Co., Ltd. (Shanghai, People's Republic of China) were used to overexpress human AIF1L in MDA-MB-231 cells via transient transfection.

Microarray and immunohistochemistry
A total of 287 tissue samples from primary BC patients who underwent curative resection were collected at the First Hospital of China Medical University between December 2003 and April 2007. Tissue specimens were initially paraffin embedded and processed for routine histological evaluation. Written informed consent was obtained from each patient. Clinicopathologic data, including age, gender, World Health Organization histological type, and TNM stage, as well as estrogen receptor (ER), progesterone receptor (PR), Ki67, and human epidermal growth factor receptor 2 (HER2) expression, were collected. A total of 259 BC patients with at least a 5-year follow-up were included in prognosis analysis. This study was conducted in accordance with the Declaration of Helsinki

and approved by the Ethics Committee of China Medical University. All samples were evaluated by two experienced pathologists to confirm diagnosis. AIF1L expression levels were detected using a two-step immunohistochemical method (Beijing Zhongshan Golden Bridge Biotechnology Company, Beijing, People's Republic of China). Rabbit polyclonal antibodies against human AIF1L were purchased from Abcam (Shanghai, People's Republic of China). Tissue microarray slides were deparaffinized in xylene and hydrated with graded alcohol before incubation with 3% H_2O_2 and heat-induced antigen retrieval. Slides were incubated with primary antibodies overnight at 4°C and stained using a two-step detection system; counterstaining was performed with hematoxylin. All procedures were carried out according to the manufacturers' instructions. For negative controls, sections were treated with 0.01 mol/L PBS instead of primary antibodies.

Cells expressing AIF1L proteins had visible brown granules in the cytoplasm and membrane. Immunostaining intensities were evaluated by two independent pathologists in a blinded manner. The scoring system was based on the intensity and extent of staining. Expression levels were classified as low and high, as previously described.[13]

Biological informatics analysis for AIF1L expression and methylation
The Cancer Genome Atlas (TCGA) RNA-sequencing database (level 3 data) included 1,100 BC samples and 112 normal controls. To identify an association between AIF1L methylation and expression, we also downloaded HumanMethylation450 data (level 3 data) for breast tumor tissues and adjacent non-tumor tissues from TCGA. The association between AIF1L mRNA expression and DNA methylation was determined by calculating the Spearman correlation coefficient. The total number of matched samples was 868. Beta-value statistics were used to measure methylation levels.[14] AIF1L protein expression in BC was confirmed according to The Human Protein Atlas.[50]

Cancer Cell Line Encyclopedia (CCLE) data analysis
The CCLE project is an effort to conduct detailed genetic characterization of a large panel of human cancer cell lines. CCLE provides public access analysis and visualization of DNA copy number, mRNA expression, mutation data, and more for ~1,000 cancer cell lines,[15,16] including 52 BC cells that were analyzed in the present study. We withdrew AIF1L co-expression genes from the CCLE database with R language, then used DAVID Bioinformatics Resources 6.7

(National Institute of Allergy and Infectious Diseases, MD, USA, National Institutes of Health [NIH]) for gene ontology and the Kyoto Encyclopedia of Genes and Genomes enrichment analyses (https://david.abcc.ncifcrf.gov/).[17,18] Data from the BC cell lines were also evaluated using gene set enrichment analysis (GSEA) and GSEA2-2.2.3 software. AIF1L expression levels were dichotomized into two groups to annotate phenotype with msigdb.v5.2.symbols gene sets.[19,20] All other parameters were set to default values.[21,22]

Transwell migration and invasion assays

Migration and invasion assays were performed as previously described.[23] For the invasion assays, 50 μL Matrigel (Corning, NY, USA) was added to the well inserts and incubated overnight. Cells (5×10^4) were suspended in serum-free culture media and seeded into Transwell inserts. Plates on the bottom received complete media and were incubated at 37°C for 24 hours. Unmigrated cells were removed using cotton swabs. Cells were fixed with 4% paraformaldehyde and stained with a 1% crystal violet solution (Sigma-Aldrich St. Louis, MO, USA). For each plate, five random fields were counted at 10× magnification. Images were processed with ImageJ software to count the number of cells in the migration and invasion assay.

Protein extraction and immunoblots

Cells were solubilized in radioimmunoprecipitation assay lysis buffer with protease inhibitors. Equal amounts of protein were resolved by sodium dodecyl sulfate-polyacrylamide gel electrophoresis and transferred to polyvinylidene fluoride membranes. Membranes were blocked with 5% nonfat milk for 2 hours and incubated overnight at 4°C with primary antibodies. Proteins were detected using an enhanced chemiluminescence kit and photographed using the ChemiDoc MP System (Bio-Rad Laboratories Inc., Hercules, CA, USA). Rabbit monoclonal antibodies against human FAK and RHOA were purchased from Abcam.

Cell spreading assays

A cell spreading assay was performed as previously described.[24] MDA-MB-231 controls and AIF1L-overexpressing cells were resuspended in serum-free medium. A total of 5×10^4 cells were added to Matrigel-coated glass coverslips. Sixty minutes after plating, cells were fixed with 4% paraformaldehyde for 20 minutes at room temperature. After washing with PBS, 0.1% Triton X-100 (in PBS) was added for 10 minutes at room temperature. Cells were blocked with 10% normal goat serum for 10 minutes at room temperature. Cells were incubated with 0.5 μM tetramethylrhodamine-phalloidin (Sigma-

Aldrich) for 1 hour at room temperature and counterstained with 4′,6-diamidino-2-phenylindole to visualize nuclei. Coverslips were imaged using epifluorescence microscopy (Nikon Corporation, Tokyo Japan). Images were processed with ImageJ software to measure the areas of the cell and nucleus. Circularity and aspect ratio were used to measure cell shape as previously described.[25,26] Both cell circularity and aspect ratio were used to measure the roundness of a cell. Over 50 cells were quantified per sample. The experiment was performed in three technical replicates.

Statistical analysis

Statistical analysis was performed with SPSS 17.0 (SPSS Inc., Chicago, IL, USA) or R language. Continuous data are shown as the mean ± SD or standard error of mean for normally distributed data. Chi-squared test or Fisher's exact test was used to compare different groups. Log-rank testing was used to assess the associations between disease-free survival and disease covariates to identify prognostic factors. Two sided $P < 0.05$ was considered statistically significant.

Results
Downregulation of AIF1L expression in BC

In this cohort, positive rates of AIF1L protein expression in BC (28.6%, 82/287) were significantly lower than in tumor-adjacent tissues (58.3%, 28/48; P=0.007; Figure 1A and B). AIF1L mRNA expression was also significantly decreased in BC compared with controls in TCGA (Figure 1E). Methylation of gene CpG island promoters is a generally accepted mechanism for silencing expression. Strong associations between methylation patterns and expression have been reported.[27] HumanMethylation450 BeadChip (450 K) is based on the Illumina Technology and contains 482,421 probes, targeting 99% of genes and 96% of CpG island regions.[28] Spearman correlation coefficients were calculated, which showed a negative correlation between the expression and methylation of *AIF1L* genes (Figure 1G). Notably, AIF1L genes were hypermethylated in tumor samples compared to normal controls (Figure 1F). Using data from Protein Atlas, AIF1L protein staining against HPA020522 and HPA056852 antibodies (rabbit polyclonal antibody; Sigma-Aldrich) was visible in both the cytoplasm and membranes. Normal breast glandular cells showed higher staining intensity for HPA020522 and medium staining intensity for HPA056852. Results of staining BC cells are as follows: medium (2/12), low (2/12), and not detected (8/12) for HPA020522 and medium (4/12), low (5/12), and not detected (3/12) for HPA056852.
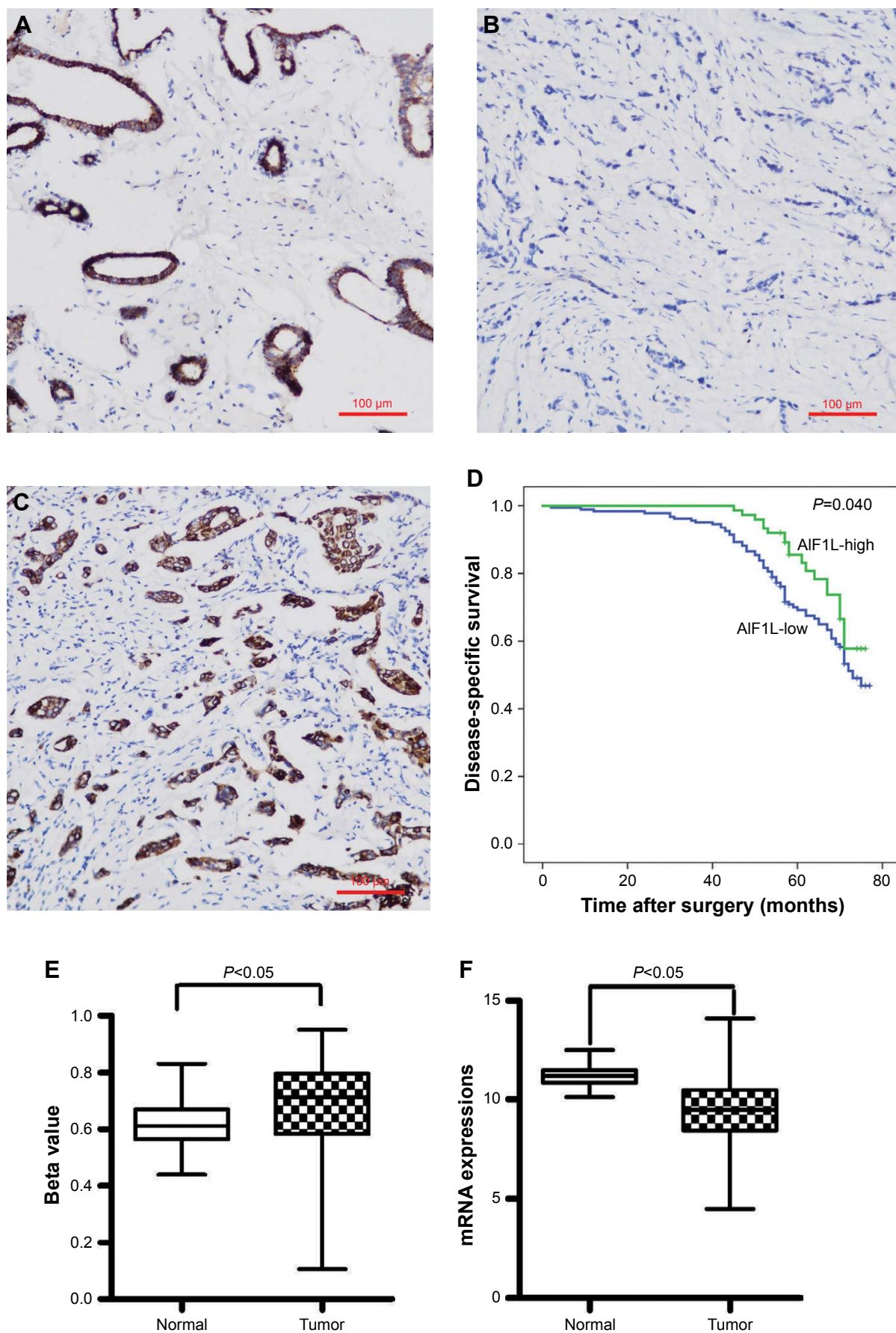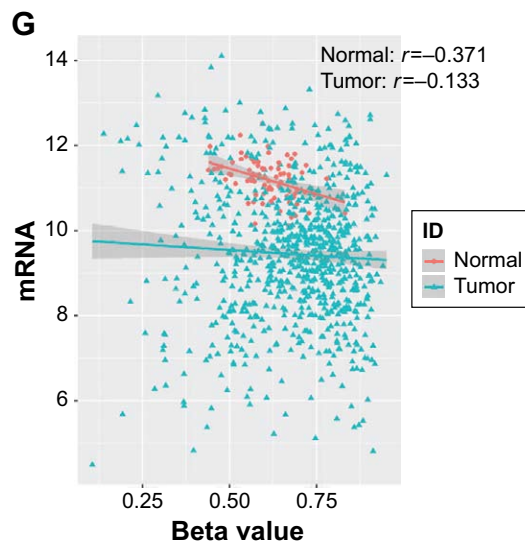
Figure 1 (*Continued*)

G

Figure 1 AIF1L expression levels in 287 surgical tissue samples from breast cancer patients were assessed by immunohistochemistry.
Notes: (**A**) Positive AIF1L staining in surrounding non-tumor areas; (**B**) Negative AIF1L staining; (**C**) Positive AIF1L staining. (**D**) Low AIF1L expression is associated with poor survival in breast cancer patients, $P=0.040$. AIF1L expression levels from TCGA. (**E**) AIF1L methylation levels were higher in breast cancer cells compared to normal controls. (**F**) AIF1L mRNA expression was lower in breast cancer cells compared to normal controls, both $P<0.05$ (P-value were calculated by t-test). (**G**) Negative correlation between AIF1L methylation levels and mRNA expression, $r=-0.371$ in normal samples; $r=-0.133$ in breast cancer samples (spearman correlation coefficient).

Correlation between AIF1L levels and clinicopathologic factors

Positive rates of AIF1L expression in HER2+ were significantly higher than HER2− ($P=0.038$). AIF1L expression was lower in triple-negative breast cancer (TNBC) compared with non-TNBC. No significant differences in AIF1L levels were detected in relation to age, T&N stage subtype, ER and PR status, and Ki67 status (Table 1).

Low expression of AIF1L correlates with shorter disease-free survival in BC patients

Patients with low AIF1L expression showed a poor disease-free survival rate ($P=0.040$; Figure 1). The hazard ratio (HR) for AIF1L protein expression was 0.610 (95% CI, 0.377–0.987; $P=0.044$) in the AIF1L-positive group (univariate analysis). Seven baseline variables (age, T&N stage subtype, ER status, PR status, HER2 status, and Ki67 status) were evaluated with AIF1L expression using Cox regression analysis. The HR for AIF1L was not significantly changed (HR=0.724 [95% CI, 0.404–1.298]; $P=0.278$).

Potential biological functions of AIF1L

To explore the unique roles of AIF1L, we identified 196 AIF1L co-expression genes from the CCLE database with R language by setting the Pearson coefficient >0.6. After performing gene ontology and the Kyoto Encyclopedia of Genes and Genomes pathway analysis using DAVID tools,[17] the most

Table 1 Clinicopathologic characteristics and AIF1L protein expression

Characteristics	n	AIF1L-low	AIF1L-high (n, %)	P-value
Age (years)				0.056
≤45	91	72	19 (20.9)	
>45	195	133	62 (31.8)	
T stage				0.35
T1	97	65	32 (33.0)	
T2	135	101	34 (25.2)	
T3	6	5	1 (16.7)	
N stage				0.331
N0	174	130	44 (25.3)	
N1	61	38	23 (37.7)	
N2	27	19	8 (29.6)	
N3	17	12	5 (29.4)	
ER status				0.339
Negative	74	56	18 (24.3)	
Positive	202	141	61 (30.2)	
PR status				0.653
Negative	78	57	21 (26.9)	
Positive	199	140	59 (29.6)	
HER2 status				0.038
Negative	246	181	65 (26.4)	
Positive	21	11	10 (47.6)	
Ki67 status				0.503
≤14%	201	144	57 (28.4)	
>14%	31	24	7 (22.6)	
Molecular subtype				
Luminal A*	158	113	45 (28.5)	0.052 (* vs $)
Luminal B#	29	19	10 (34.5)	0.038 (# vs $)
TNBC$	38	33	5 (13.2)	
HER2+&	12	6	6 (50)	0.007 (& vs $)

Notes: *Luminal A; #Luminal B; $TNBC; &HER2+.
Abbreviations: ER, estrogen receptor; HER2, human epidermal growth factor receptor 2; PR, progesterone receptor; TNBC, triple-negative breast cancer.
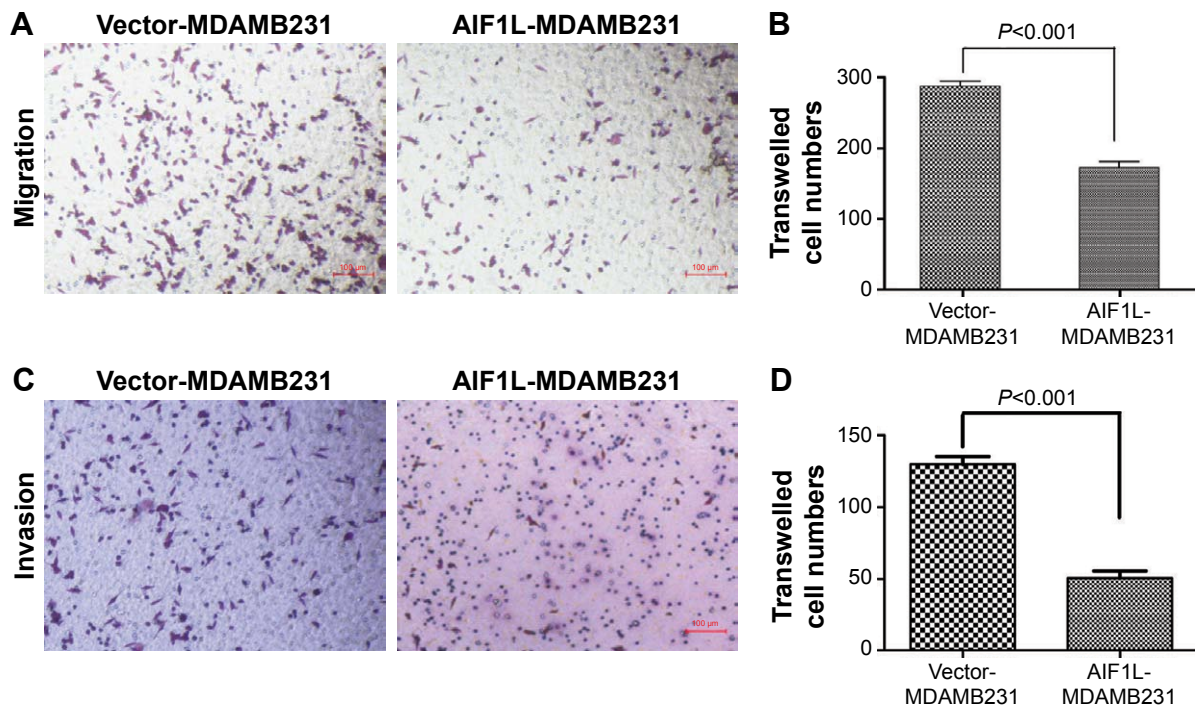
enriched biological themes were related to tight junctions and cell junctions (Figure 2A). To further assess the biological function of AIF1L in breast tumorigenesis, we applied GSEA to BC cells from the CCLE. Top 50 differentially expressed genes between low vs high expressions of AIF1L are shown in Table S1. Downregulation of AIF1L was significantly correlated with focal adhesion (FA; Figure 2B). Genes in the FA pathway were identified by GSEA (Figure 2C; Table S2).

AIF1L inhibits migration and invasion of MDA-MB-231 BC cells

The mRNA expression levels of BC cells in CCLE are shown Figure S1. AIF1L expression of MDA-MB-231 cells was lower than that of immortalized epithelial HMEL cells. To further investigate the effect of AIF1L overexpression on cell migration and invasion, the Transwell migration and invasion assays were performed. Transwell migration and invasion assays showed that transient overexpression of AIF1L significantly suppressed migration and invasion compared to the control group ($P<0.05$; Figure 3).

AIF1L inhibits MDA-MB-231 cell spreading and mediates focal adhesion kinase (FAK) levels involved in ROCK signaling

Cell migration and spreading are initiated by global reorganization of the actin cytoskeleton and extending actin polymerization-driven lamellipodium protrusions of the cell membrane.[29,30] Thirty minutes after plating, cells overexpressing AIF1L spread less efficiently than the control cells (Figure 4A, B, E) and were less elongated, as indicated by an increase in circularity and decrease in aspect ratio (Figure 4C–F). Elongated cells showed actin remodeling toward the membrane, which is equivalent to the formation of ruffles and pseudopodia (Figure 4D).

A

Annotation cluster	Enrichment score: 5.3263843074630515	Count	%	P-value
Category	**Term**			
UP_KEYWORDS	Tight junction	10	5.46	6.63E-08
GOTERM_CC_DIRECT	GO:0005923~tight junction	11	6.01	1.29E-07
GOTERM_BP_DIRECT	GO:0070830~tight junction assembly	6	3.27	1.32E-05
UP_KEYWORDS	Cell junction	18	9.83	1.01E-04
KEGG_PATHWAY	hsa04530~tight junction	8	4.37	2.05E-04

B

Enrichment score	0.6287439
Nominal *P*-value	0.0
FDR *q* value	0.5951533

C

Figure 2 Gene set enrichment analysis (GSEA) and DAVID functional annotation clustering using public repository data from CCLE.
Notes: (**A**) DAVID functional annotation clustering for AIF1L co-expression genes. (**B**) GSEA for HSA04510_FOCAL_ADHESION, which is related to low AIF1L expression. (**C**) Genes in the HSA04510_FOCAL_ADHESION pathway are upregulated in breast cancer cells with low AIF1L levels.
Abbreviation: FDR, false discovery rate.

Figure 3 Decreased migration and invasion of MDAMB-231 cells with transient AIF1L overexpression.
Notes: Cell migration (**A**) and invasion (**C**) were detected using transwell assays. Representative images are shown following staining with crystal violet. Quantification of cell migration (**B**) and invasion (**D**) are also shown.

FAK is a nonreceptor tyrosine kinase that plays a central role in cell migration through regulation of lamellipodial formation and FAs.[31,32] Increased FAK expression has been correlated with increased clinical progression in BC.[33,34] Therefore, we assessed FAK expression in AIF1L-overexpressing MDA-MB-231 cells and controls and showed that AIF1L led to increased inhibition of FAK expression (Figure 4G). FAK is involved with activators and/or inhibitors of the small GTPase RhoA that enable FAK activity to be connected to alterations in polymerization of actin filaments during tumor cell adhesion and motility.[35,36] RhoA expression was also inhibited by AIF1L overexpression in MDA-MB-231 cells (Figure 4G).

Discussion

In the present study, we analyzed the expression and clinicopathologic significance of AIF1L in BC. Low AIF1L protein expression was observed in 71.4% of BC samples in this cohort. AIF1L mRNA expression was also lower in patients with BC in TCGA cohort. Furthermore, AIF1L protein expression in BC was confirmed from Protein Atlas. Thus, AIF1L expression is downregulated in BC. Furthermore, we integrated AIF1L DNA methylation and gene expression from TCGA database and found that AIF1L downregulation may be due to hypermethylation of the promoter. Given that the Spearman correlation coefficient was very low, particularly

with tumor tissues, we searched[51] and found that no genetic alterations in AIF1L were reported in 977 sequenced patients from TCGA. We hypothesized that in addition to methylation, there might be some other reason for AIF1L downregulation, such as a posttranscriptional regulation mechanism rather than gene mutation. Low AIF1L expression was detected in TNBC and was correlated with a poor postoperative disease-specific survival. TNBC accounts for ~15%–20% of BCs and is defined by the absence of ERα, PR, and HER2 amplification, which is resistant to conventional chemotherapy, lack of targeting agents and is often associated with a poor prognosis.[37,38] AIF1L could be a unique molecular target of TNBCs.

CCLE data analysis revealed AIF1L-related pathways, including cell junction, tight junction, and FA. Of the AIF1L co-expression genes, CDH1 (cadherin 1, E-cadherin) is a major component of intercellular junctions, and loss of its expression has been shown to reduce BC invasion and metastasis.[39,40] FAs connect the cytoskeleton and extracellular matrix (ECM). Interplay between the actin cytoskeleton and FA dynamics results in a balance between adhesion and contraction, which greatly influences cell migration.[35,41]

Although AIF1L induces cytoskeletal rearrangements in HeLa cells and podocytes, whether it is involved in BC progression, especially in TNBCs, is not understood. The data reported herein show that ectopic AIF1L expression suppresses MDA-MB-231 BC cell motility and invasion
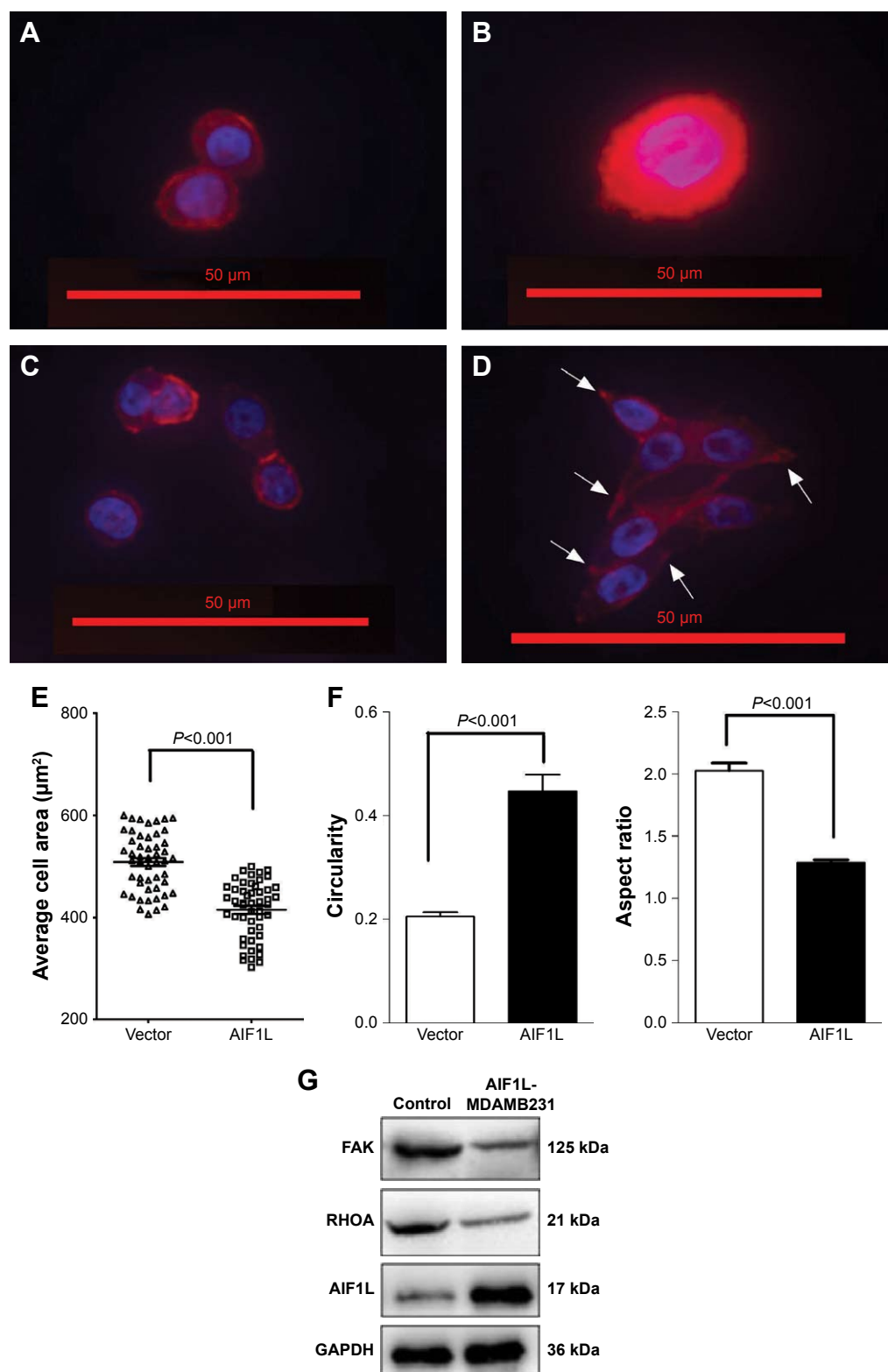
Figure 4 AIF1L inhibits cell spreading and alters cell morphology.
Notes: (**A**, **B**) AIF1L overexpression in MDA-MB-231 cells resulted in slower spreading on a matrigel coated surface compared with controls. Representative images of cells stained using TRITC-phalloidin and DAPI to show the nuclei. (**C**, **D**) Example images of rounded cells and elongated cells. (**E**) Average area of cells ± SEM from a minimum of 50 cells for each treatment. (**F**) Cell circularity and aspect ratio were measured from at least 50 cells for AIF1L overexpression in MDA-MB-231 cells and controls. AIF1L increased circularity and reduced the aspect ratio on a matrigel coated surface compared with controls. Arrows show cell protrusions. Statistical significance was evaluated using the two-sample t-test: *$P<0$ .05. (**G**) A representative Western blot demonstrating downregulation of FAK and RHOA expression in MDA-MB-231 cells overexpressing AIF1L.

by inducing cytoskeletal modifications, which are achieved through FAK/RHOA signaling. High FAK expression was correlated with shorter overall survival and progression-free survival in patients with BC, especially in TNBC patients with high FAK expression.[42,43] RhoA protein is also overexpressed in BC.[44,45] The actin cytoskeleton is linked to invasive and metastatic phenotypes of malignant cancer cells. Cell migration is driven by cycles of actin polymerization and is initiated by cell membrane protrusions called filopodia, lamellipodia, and invadopodia.[46] These protrusions are stabilized by adhesions linking the actin cytoskeleton to ECM proteins and actomyosin contraction.[35,47] Located on the inner face of the cell membrane, FAs form a vital link between the ECM and the cytoskeleton. Interplay between F-actin contractile forces and FA dynamics greatly influences cell migration capacity.[35] Integrin receptor binding to ECM proteins is one of the strongest activators of FAK.[48,49] In the present study, MDA-MB-231 cells transfected with AIF1L showed decreased cell spreading, more circular cell shape, and formation of fewer protrusions. GSEA also found low AIF1L expression correlated with high expression of collagens such as COL4, COL6, COL5, and COL1. AIF1L may inhibit FAK/RHOA expression through interfering in cell–ECM signaling. But the accurate molecular mechanism needs further research. These results support a role for AIF1L in regulating actin remodeling associated with cell migration.

Conclusion

This study evaluated AIF1L expression in BC and found that AIF1L downregulation may predict a poor prognosis. AIF1L suppresses BC migration and invasion through regulating actin remodeling, which is dependent on FAK/RHOA signaling. However, additional mechanisms that influence AIF1L regulation of the actin cytoskeleton should be identified and characterized in the future.

Disclosure

The authors report no conflicts of interest in this work.

References

1. Torre LA, Bray F, Siegel RL, Ferlay J, Lortet-Tieulent J, Jemal A. Global cancer statistics, 2012. *CA Cancer J Clin*. 2015;65(2):87–108.
2. Ginsburg O, Bray F, Coleman MP, et al. The global burden of women's cancers: a grand challenge in global health. *Lancet*. 2017;389(10071):847–860.
3. Kawasaki H, Kretsinger RH. Structural and functional diversity of EF-hand proteins: Evolutionary perspectives. *Protein Sci*. 2017;26(10):1898–1920.
4. Clapham DE. Calcium signaling. *Cell*. 2007;131(6):1047–1058.
5. Schulze JO, Quedenau C, Roske Y, et al. Structural and functional characterization of human Iba proteins. *FEBS J*. 2008;275(18):4627–4640.
6. Ito D, Imai Y, Ohsawa K, Nakajima K, Fukuuchi Y, Kohsaka S. Microglia-specific localisation of a novel calcium binding protein, Iba1. *Brain Res Mol Brain Res*. 1998;57(1):1–9.
7. Yang ZF, Ho DW, Lau CK, et al. Allograft inflammatory factor-1 (AIF-1) is crucial for the survival and pro-inflammatory activity of macrophages. *Int Immunol*. 2005;17(11):1391–1397.
8. Autieri MV, Kelemen S, Thomas BA, Feller ED, Goldman BI, Eisen HJ. Allograft inflammatory factor-1 expression correlates with cardiac rejection and development of cardiac allograft vasculopathy. *Circulation*. 2002;106(17):2218–2223.
9. Cai H, Zhu XD, Ao JY, Jy A, et al. Colony-stimulating factor-1-induced AIF1 expression in tumor-associated macrophages enhances the progression of hepatocellular carcinoma. *Oncoimmunology*. 2017;6(9):e1333213.
10. Uhlen M, Zhang C, Lee S, et al. A pathology atlas of the human cancer transcriptome. *Science*. 2017;357(6352):eaan2507.
11. Uhlén M, Fagerberg L, Hallström BM, et al. Proteomics. Tissue-based map of the human proteome. *Science*. 2015;347(6220):1260419.
12. Lu Y, Ye Y, Bao W, et al. Genome-wide identification of genes essential for podocyte cytoskeletons based on single-cell RNA sequencing. *Kidney Int*. 2017;92(5):1119–1129.
13. Zhang H, Luo M, Jin Z, et al. Expression and clinicopathological significance of FSIP1 in breast cancer. *Oncotarget*. 2015;6(12):10658–10666.
14. Du P, Zhang X, Huang CC, et al. Comparison of Beta-value and M-value methods for quantifying methylation levels by microarray analysis. *BMC Bioinformatics*. 2010;11:587.
15. Barretina J, Caponigro G, Stransky N, et al. The Cancer Cell Line Encyclopedia enables predictive modelling of anticancer drug sensitivity. *Nature*. 2012;483(7391):603–607.
16. Shiau CK, Gu DL, Chen CF, Lin CH, Jou YS. IGRhCellID: integrated genomic resources of human cell lines for identification. *Nucleic Acids Res*. 2011;39(Database issue):D520–D524.
17. Huang da W, Sherman BT, Lempicki RA. Systematic and integrative analysis of large gene lists using DAVID bioinformatics resources. *Nat Protoc*. 2009;4(1):44–57.
18. Huang da W, Sherman BT, Lempicki RA. Bioinformatics enrichment tools: paths toward the comprehensive functional analysis of large gene lists. *Nucleic Acids Res*. 2009;37(1):1–13.
19. Liberzon A, Subramanian A, Pinchback R, Thorvaldsdóttir H, Tamayo P, Mesirov JP. Molecular signatures database (MSigDB) 3.0. *Bioinformatics*. 2011;27(12):1739–1740.
20. Liberzon A, Birger C, Thorvaldsdóttir H, Ghandi M, Mesirov JP, Tamayo P. The Molecular Signatures Database (MSigDB) hallmark gene set collection. *Cell Syst*. 2015;1(6):417–425.
21. Subramanian A, Tamayo P, Mootha VK, et al. Gene set enrichment analysis: a knowledge-based approach for interpreting genome-wide expression profiles. *Proc Natl Acad Sci U S A*. 2005;102(43):15545–15550.
22. Mootha VK, Lindgren CM, Eriksson KF, et al. PGC-1alpha-responsive genes involved in oxidative phosphorylation are coordinately downregulated in human diabetes. *Nat Genet*. 2003;34(3):267–273.
23. Xiong X, Wang Y, Liu C, et al. Heat shock protein 90β stabilizes focal adhesion kinase and enhances cell migration and invasion in breast cancer cells. *Exp Cell Res*. 2014;326(1):78–89.
24. Humphries MJ. Cell adhesion assays. *Methods Mol Biol*. 2009;522:203–210.
25. Carey SP, Kraning-Rush CM, Williams RM, Reinhart-King CA. Biophysical control of invasive tumor cell behavior by extracellular matrix microarchitecture. *Biomaterials*. 2012;33(16):4157–4165.
26. Gehler S, Compere FV, Miller AM. Semaphorin 3A increases FAK phosphorylation at focal adhesions to modulate MDA-MB-231 cell migration and spreading on different substratum concentrations. *Int J Breast Cancer*. 2017;2017:9619734.
27. Vanderkraats ND, Hiken JF, Decker KF, Edwards JR. Discovering high-resolution patterns of differential DNA methylation that correlate with gene expression changes. *Nucleic Acids Res*. 2013;41(14):6816–6827.

28. Bibikova M, Barnes B, Tsan C, et al. High density DNA methylation array with single CpG site resolution. *Genomics*. 2011;98(4):288–295.

29. Parsons JT, Horwitz AR, Schwartz MA. Cell adhesion: integrating cytoskeletal dynamics and cellular tension. *Nat Rev Mol Cell Biol*. 2010;11(9):633–643.

30. Zimerman B, Volberg T, Geiger B. Early molecular events in the assembly of the focal adhesion-stress fiber complex during fibroblast spreading. *Cell Motil Cytoskeleton*. 2004;58(3):143–159.

31. Mitra SK, Hanson DA, Schlaepfer DD. Focal adhesion kinase: in command and control of cell motility. *Nat Rev Mol Cell Biol*. 2005; 6(1):56–68.

32. Mitra SK, Schlaepfer DD. Integrin-regulated FAK-Src signaling in normal and cancer cells. *Curr Opin Cell Biol*. 2006;18(5):516–523.

33. Almstedt K, Sicking I, Battista MJ, et al. Prognostic significance of focal adhesion kinase in node-negative breast cancer. *Breast Care*. 2017;12(5):329–333.

34. Lark AL, Livasy CA, Dressler L, et al. High focal adhesion kinase expression in invasive breast carcinomas is associated with an aggressive phenotype. *Mod Pathol*. 2005;18(10):1289–1294.

35. Fife CM, Mccarroll JA, Kavallaris M. Movers and shakers: cell cytoskeleton in cancer metastasis. *Br J Pharmacol*. 2014;171(24):5507–5523.

36. Lim Y, Lim ST, Tomar A, et al. PyK2 and FAK connections to p190Rho guanine nucleotide exchange factor regulate RhoA activity, focal adhesion formation, and cell motility. *J Cell Biol*. 2008;180(1): 187–203.

37. Papa A, Caruso D, Tomao S, Rossi L, Zaccarelli E, Tomao F. Triple-negative breast cancer: investigating potential molecular therapeutic target. *Expert Opin Ther Targets*. 2015;19(1):55–75.

38. Arnedos M, Bihan C, Delaloge S, Andre F. Triple-negative breast cancer: are we making headway at least? *Ther Adv Med Oncol*. 2012; 4(4):195–210.

39. Onder TT, Gupta PB, Mani SA, Yang J, Lander ES, Weinberg RA. Loss of E-cadherin promotes metastasis via multiple downstream transcriptional pathways. *Cancer Res*. 2008;68(10):3645–3654.

40. Derksen PW, Liu X, Saridin F, et al. Somatic inactivation of E-cadherin and p53 in mice leads to metastatic lobular mammary carcinoma through induction of anoikis resistance and angiogenesis. *Cancer Cell*. 2006;10(5):437–449.

41. Gupton SL, Waterman-Storer CM. Spatiotemporal feedback between actomyosin and focal-adhesion systems optimizes rapid cell migration. *Cell*. 2006;125(7):1361–1374.

42. Golubovskaya VM, Ylagan L, Miller A, et al. High focal adhesion kinase expression in breast carcinoma is associated with lymphovascular invasion and triple-negative phenotype. *BMC Cancer*. 2014;14:769.

43. Yom CK, Noh DY, Kim WH, Kim HS. Clinical significance of high focal adhesion kinase gene copy number and overexpression in invasive breast cancer. *Breast Cancer Res Treat*. 2011;128(3):647–655.

44. Murakami E, Nakanishi Y, Hirotani Y, et al. Roles of Ras homolog A in invasive ductal breast carcinoma. *Acta Histochem Cytochem*. 2016; 49(5):131–140.

45. Bellizzi A, Mangia A, Chiriatti A, et al. RhoA protein expression in primary breast cancers and matched lymphocytes is associated with progression of the disease. *Int J Mol Med*. 2008;22(1):25–31.

46. Yamaguchi H, Condeelis J. Regulation of the actin cytoskeleton in cancer cell migration and invasion. *Biochim Biophys Acta*. 2007; 1773(5):642–652.

47. Olson MF, Sahai E. The actin cytoskeleton in cancer cell motility. *Clin Exp Metastasis*. 2009;26(4):273–287.

48. Kanchanawong P, Shtengel G, Pasapera AM, et al. Nanoscale architecture of integrin-based cell adhesions. *Nature*. 2010;468(7323):580–584.

49. Horton ER, Byron A, Askari JA, et al. Definition of a consensus integrin adhesome and its dynamics during adhesion complex assembly and disassembly. *Nat Cell Biol*. 2015;17(12):1577–1587.

50. Uhlén M, Fagerberg L, Hallström BM, et al. Proteomics. Tissue-based map of the human proteome. *Science*. 2015;347(6220):1260419.

51. Gao J, Aksoy BA, Dogrusoz U, et al. Integrative analysis of complex cancer genomics and clinical profiles using the cBioPortal. *Sci Signal*. 2013;2:6(269):1.

Supplementary materials

Table S1 Differentially expressed genes between low vs high expressions of AIF1L gene in CCLE breast cell database

Name	Gene_symbol	Gene_title	Score
FOSL1	FOSL1	FOS-like antigen 1	0.837046
EMP3	EMP3	Epithelial membrane protein 3	0.802068
ZDHHC2	ZDHHC2	Zinc finger, DHHC-type containing 2	0.790615
AXL	AXL	AXL receptor tyrosine kinase	0.781382
IGFBP7	IGFBP7	Insulin-like growth factor binding protein 7	0.76961
SERPINE1	SERPINE1	Serpin peptidase inhibitor, clade E (nexin, plasminogen activator inhibitor type 1), member 1	0.75092
COL4A2	COL4A2	Collagen, type IV, alpha 2	0.746052
TGFB1I1	TGFB1I1	Transforming growth factor beta 1 induced transcript 1	0.729768
IGFBP6	IGFBP6	Insulin-like growth factor binding protein 6	0.725726
COL4A1	COL4A1	Collagen, type IV, alpha 1	0.707212
HRH1	HRH1	Histamine receptor H1	0.690314
BCAT1	BCAT1	Branched chain aminotransferase 1, cytosolic	0.685178
PROCR	PROCR	Protein C receptor, endothelial (EPCR)	0.684549
COL6A2	COL6A2	Collagen, type VI, alpha 2	0.667416
PHLDA1	PHLDA1	Pleckstrin homology-like domain, family A, member 1	0.667399
SLFN12	SLFN12	Schlafen family member 12	0.663343
RAB34	RAB34	RAB34, member RAS oncogene family	0.646708
PLAU	PLAU	Plasminogen activator, urokinase	0.640417
AKAP12	AKAP12	A kinase (PRKA) anchor protein (gravin) 12	0.630199
DFNA5	DFNA5	Deafness, autosomal dominant 5	0.629837
LHFP	LHFP	Lipoma HMGIC fusion partner	0.627571
SPOCK1	SPOCK1	Sparc/osteonectin, cwcv and kazal-like domains proteoglycan (testican) 1	0.622842
FAM101B	FAM101B	Family with sequence similarity 101, member B	0.619061
COL6A1	COL6A1	Collagen, type VI, alpha 1	0.611874
ADAM19	ADAM19	ADAM metallopeptidase domain 19 (meltrin beta)	0.610056
COL5A2	COL5A2	Collagen, type V, alpha 2	0.607276
TIMP1	TIMP1	TIMP metallopeptidase inhibitor 1	0.606783
SCG2	SCG2	Secretogranin II (chromogranin C)	0.60473
NOV	NOV	Nephroblastoma overexpressed gene	0.604233
TMEM158	TMEM158	Transmembrane protein 158	0.603507
DKK3	DKK3	Dickkopf homolog 3 (Xenopus laevis)	0.602322
PRR16	PRR16	Proline rich 16	0.599183
IL6	IL6	Interleukin 6 (interferon, beta 2)	0.598937
LIF	LIF	Leukemia inhibitory factor (cholinergic differentiation factor)	0.597241
FGF2	FGF2	Fibroblast growth factor 2 (basic)	0.596823
TNFAIP3	TNFAIP3	Tumor necrosis factor, alpha-induced protein 3	0.595126
GLIS3	GLIS3	GLIS family zinc finger 3	0.594521
EPHA2	EPHA2	EPH receptor A2	0.593322
NT5E	NT5E	5′-nucleotidase, ecto (CD73)	0.586506
TMEM22	TMEM22	Transmembrane protein 22	0.586264
FYN	FYN	FYN oncogene related to SRC, FGR, YES	0.584119
PTRF	PTRF	Polymerase I and transcript release factor	0.583833
MMP2	MMP2	Matrix metallopeptidase 2 (gelatinase A, 72 kDa gelatinase, 72 kDa type IV collagenase)	0.583674
TMEM133	TMEM133	Transmembrane protein 133	0.582601
PTPRM	PTPRM	Protein tyrosine phosphatase, receptor type, M	0.580363
IGF2BP3	IGF2BP3	Insulin-like growth factor 2 mRNA binding protein 3	0.57938
FBN1	FBN1	Fibrillin 1	0.576254
CAV1	CAV1	Caveolin 1, caveolae protein, 22 kDa	0.575581
CDH2	CDH2	Cadherin 2, type 1, N-cadherin (neuronal)	0.573586
FSTL1	FSTL1	Follistatin-like 1	0.571101
FGF13	FGF13	Fibroblast growth factor 13	−0.44624
CYP4X1	CYP4X1	Cytochrome P450, family 4, subfamily X, polypeptide 1	−0.44881

(Continued)

Table S1 (*Continued*)

Name	Gene_symbol	Gene_title	Score
PRSS8	PRSS8	Protease, serine 8 (prostasin)	−0.44885
HRASLS	HRASLS	HRAS-like suppressor	−0.4543
CDH1	CDH1	Cadherin 1, type 1, E-cadherin (epithelial)	−0.45663
SYCP2	SYCP2	Synaptonemal complex protein 2	−0.45812
ZNF138	ZNF138	Zinc finger protein 138	−0.45815
REPS2	REPS2	RALBP1-associated Eps domain containing 2	−0.46265
C19orf46	C19ORF46	Chromosome 19 open reading frame 46	−0.46353
VTCN1	VTCN1	V-set domain containing T cell activation inhibitor 1	−0.46819
C1orf172	C1ORF172	Chromosome 1 open reading frame 172	−0.46911
MAPT	MAPT	Microtubule-associated protein tau	−0.47075
IGSF9	IGSF9	Immunoglobulin superfamily, member 9	−0.47255
C9orf152	C9ORF152	Chromosome 9 open reading frame 152	−0.47257
RAB25	RAB25	RAB25, member RAS oncogene family	−0.4732
KIAA1324	KIAA1324	KIAA1324	−0.4738
FOXA1	FOXA1	Forkhead box A1	−0.47381
SPDEF	SPDEF	SAM pointed domain containing ets transcription factor	−0.47942
REEP1	REEP1	Receptor accessory protein 1	−0.48044
CGN	CGN	Cingulin	−0.48205
OAZ3	OAZ3	Ornithine decarboxylase antizyme 3	−0.48362
MB	MB	myoglobin	−0.48515
NEBL	NEBL	Nebulette	−0.48792
ST6GAL1	ST6GAL1	ST6 beta-galactosamide alpha-2,6-sialyltranferase 1	−0.49266
ALDH3B2	ALDH3B2	Aldehyde dehydrogenase 3 family, member B2	−0.49449
CLDN4	CLDN4	Claudin 4	−0.49664
LOC100506497	Null	Null	−0.50289
GRHL2	GRHL2	Grainyhead-like 2 (*Drosophila*)	−0.50291
CLDN3	CLDN3	Claudin 3	−0.50757
ZNF467	ZNF467	Zinc finger protein 467	−0.50862
SIDT1	SIDT1	SID1 transmembrane family, member 1	−0.51057
CEBPA	CEBPA	CCAAT/enhancer binding protein (C/EBP), alpha	−0.51303
BSPRY	BSPRY	B-box and SPRY domain containing	−0.51612
RASEF	RASEF	RAS and EF-hand domain containing	−0.5214
IRX5	IRX5	Iroquois homeobox protein 5	−0.52766
EPN3	EPN3	Epsin 3	−0.53665
EFNA3	EFNA3	Ephrin-A3	−0.54208
SELENBP1	SELENBP1	Selenium binding protein 1	−0.54401
GLYATL2	GLYATL2	Glycine-*N*-acyltransferase-like 2	−0.54889
GRHL1	GRHL1	Grainyhead-like 1 (*Drosophila*)	−0.5533
CRABP2	CRABP2	Cellular retinoic acid binding protein 2	−0.55677
HEY2	HEY2	Hairy/enhancer-of-split related with YRPW motif 2	−0.56036
TFAP2C	TFAP2C	Transcription factor AP-2 gamma (activating enhancer binding protein 2 gamma)	−0.5666
RERG	RERG	RAS-like, estrogen-regulated, growth inhibitor	−0.56686
SYT12	SYT12	Synaptotagmin XII	−0.57878
CYP4Z1	CYP4Z1	Cytochrome P450, family 4, subfamily Z, polypeptide 1	−0.61774
EFHD1	EFHD1	EF-hand domain family, member D1	−0.62168
PRLR	PRLR	Prolactin receptor	−0.62633
MYB	MYB	v-myb myeloblastosis viral oncogene homolog (avian)	−0.6605
VAV3	VAV3	vav 3 oncogene	−0.75064

Abbreviation: CCLE, Cancer Cell Line Encyclopedia.

Table S2 The most affected genes in the HSA04510_FOCAL_ADHESION pathway

Name	Gene_symbol	Gene_title	Rank in gene list	Rank metric score	Running es
row_0	COL4A2	Collagen, type IV, alpha 2	6	0.746052	0.024102
row_1	COL4A1	Collagen, type IV, alpha 1	9	0.707211	0.047146
row_2	COL6A2	Collagen, type VI, alpha 2	13	0.667416	0.068834
row_3	COL6A1	Collagen, type VI, alpha 1	25	0.611874	0.088276
row_4	COL5A2	Collagen, type V, alpha 2	27	0.607276	0.108102
row_5	FYN	FYN oncogene related to SRC, FGR, YES	45	0.584118	0.126316
row_6	CAV1	Caveolin 1, caveolae protein, 22 kDa	52	0.575581	0.144838
row_7	VEGFC	Vascular endothelial growth factor C	72	0.553132	0.161931
row_8	COL1A2	Collagen, type I, alpha 2	81	0.540925	0.179211
row_9	AKT3	v-akt murine thymoma viral oncogene homolog 3 (protein kinase B, gamma)	117	0.493746	0.193506
row_10	ITGA4	Integrin, alpha 4 (antigen CD49D, alpha 4 subunit of VLA-4 receptor)	145	0.472133	0.20752
row_11	FLNC	Filamin C, gamma (actin binding protein 280)	200	0.44223	0.219114
row_12	LAMC2	Laminin, gamma 2	203	0.441652	0.233465
row_13	CAV2	Caveolin 2	215	0.436721	0.247174
row_14	LAMA4	Laminin, alpha 4	225	0.433796	0.260894
row_15	BIRC3	Baculoviral IAP repeat-containing 3	226	0.433145	0.275073
row_16	ITGA3	Integrin, alpha 3 (antigen CD49C, alpha 3 subunit of VLA-3 receptor)	235	0.427453	0.288639
row_17	ITGA5	Integrin, alpha 5 (fibronectin receptor, alpha polypeptide)	241	0.425145	0.302289
row_18	COL3A1	Collagen, type III, alpha 1 (Ehlers–Danlos syndrome type IV, autosomal dominant)	278	0.406763	0.313683
row_19	ITGA6	Integrin, alpha 6	282	0.405993	0.326814
row_20	LAMB3	Laminin, beta 3	287	0.403633	0.339813
row_21	PDGFC	Platelet-derived growth factor C	299	0.400535	0.352338
row_22	LAMC1	Laminin, gamma 1 (formerly LAMB2)	346	0.382794	0.362413
row_23	FN1	Fibronectin 1	360	0.376867	0.374056
row_24	COL5A1	Collagen, type V, alpha 1	365	0.375251	0.386127
row_25	MYL9	Myosin, light chain 9, regulatory	369	0.373747	0.398201
row_26	MYLK	Myosin, light chain kinase	387	0.368815	0.409367
row_27	PDGFA	Platelet-derived growth factor alpha polypeptide	501	0.33853	0.414418
row_28	PIK3CD	Phosphoinositide-3-kinase, catalytic, delta polypeptide	531	0.329876	0.423668
row_29	LAMB1	Laminin, beta 1	532	0.329803	0.434465
row_30	PRKCA	Protein kinase C, alpha	533	0.329702	0.445257
row_31	COL1A1	Collagen, type I, alpha 1	536	0.329197	0.455927
row_32	ITGB4	Integrin, beta 4	581	0.321616	0.464107
row_33	LAMA2	Laminin, alpha 2 (merosin, congenital muscular dystrophy)	586	0.320621	0.474389
row_34	COL6A3	Collagen, type VI, alpha 3	588	0.32032	0.484821
row_35	MET	met proto-oncogene (hepatocyte growth factor receptor)	604	0.316587	0.494384
row_36	THBS1	Thrombospondin 1	698	0.297631	0.499164
row_37	COL4A6	Collagen, type IV, alpha 6	749	0.288689	0.505945
row_38	SPP1	Secreted phosphoprotein 1 (osteopontin, bone sialoprotein I, early T-lymphocyte activation 1)	782	0.281494	0.513452
row_39	LAMB2	Laminin, beta 2 (laminin S)	838	0.268912	0.519319
row_40	PARVA	Parvin, alpha	880	0.259453	0.525624
row_41	PDGFRB	Platelet-derived growth factor receptor, beta polypeptide	915	0.25332	0.532102
row_42	PGF	Placental growth factor, vascular endothelial growth factor-related protein	998	0.241213	0.535622
row_43	ACTN1	Actinin, alpha 1	1,007	0.240274	0.54306
row_44	TNC	Tenascin C (hexabrachion)	1,012	0.239859	0.550698
row_45	FLNA	Tilamin A, alpha (actin-binding protein 280)	1,066	0.23099	0.555431
row_46	RAC2	ras-related C3 botulinum toxin substrate 2 (rho family, small GTP binding protein Rac2)	1,087	0.227534	0.561812
row_47	PARVB	Parvin, beta	1,129	0.222995	0.566924
row_48	TLN1	Talin 1	1,239	0.209093	0.567951
row_49	VCL	Vinculin	1,253	0.2071	0.574036
row_50	ZYX	Zyxin	1,275	0.204779	0.579619
row_51	COL5A3	Collagen, type V, alpha 3	1,409	0.19049	0.578756
row_52	PXN	Paxillin	1,482	0.184277	0.580945
row_53	COL11A1	Collagen, type XI, alpha 1	1,517	0.180528	0.58504

(*Continued*)

Table S2 (*Continued*)

| Name	Gene_symbol	Gene_title	Rank in gene list	Rank metric score	Running es
row_54	CAPN2	Calpain 2, (m/II) large subunit	1,554	0.176329	0.588891
row_55	LAMA1	Laminin, alpha 1	1,609	0.170144	0.591579
row_56	ACTN4	Actinin, alpha 4	1,645	0.16764	0.595198
row_57	ITGAV	Integrin, alpha V (vitronectin receptor, alpha polypeptide, antigen CD51)	1,728	0.160049	0.596061
row_58	PDGFRA	Platelet-derived growth factor receptor, alpha polypeptide	1,742	0.158875	0.600568
row_59	ITGA8	Integrin, alpha 8	1,754	0.158028	0.605154
row_60	SHC3	SHC (Src homology 2 domain containing) transforming protein 3	1,763	0.157112	0.60987
row_61	ITGA11	Integrin, alpha 11	1,768	0.15679	0.614789
row_62	SHC1	SHC transforming protein 1	1,818	0.153003	0.617182
row_63	THBS2	Thrombospondin 2	1,826	0.152263	0.621793
row_64	CCND1	Cyclin D1	1,879	0.149562	0.623914
row_65	ITGA2	Integrin, alpha 2 (CD49B, alpha 2 subunit of VLA-2 receptor)	1,881	0.14919	0.628744
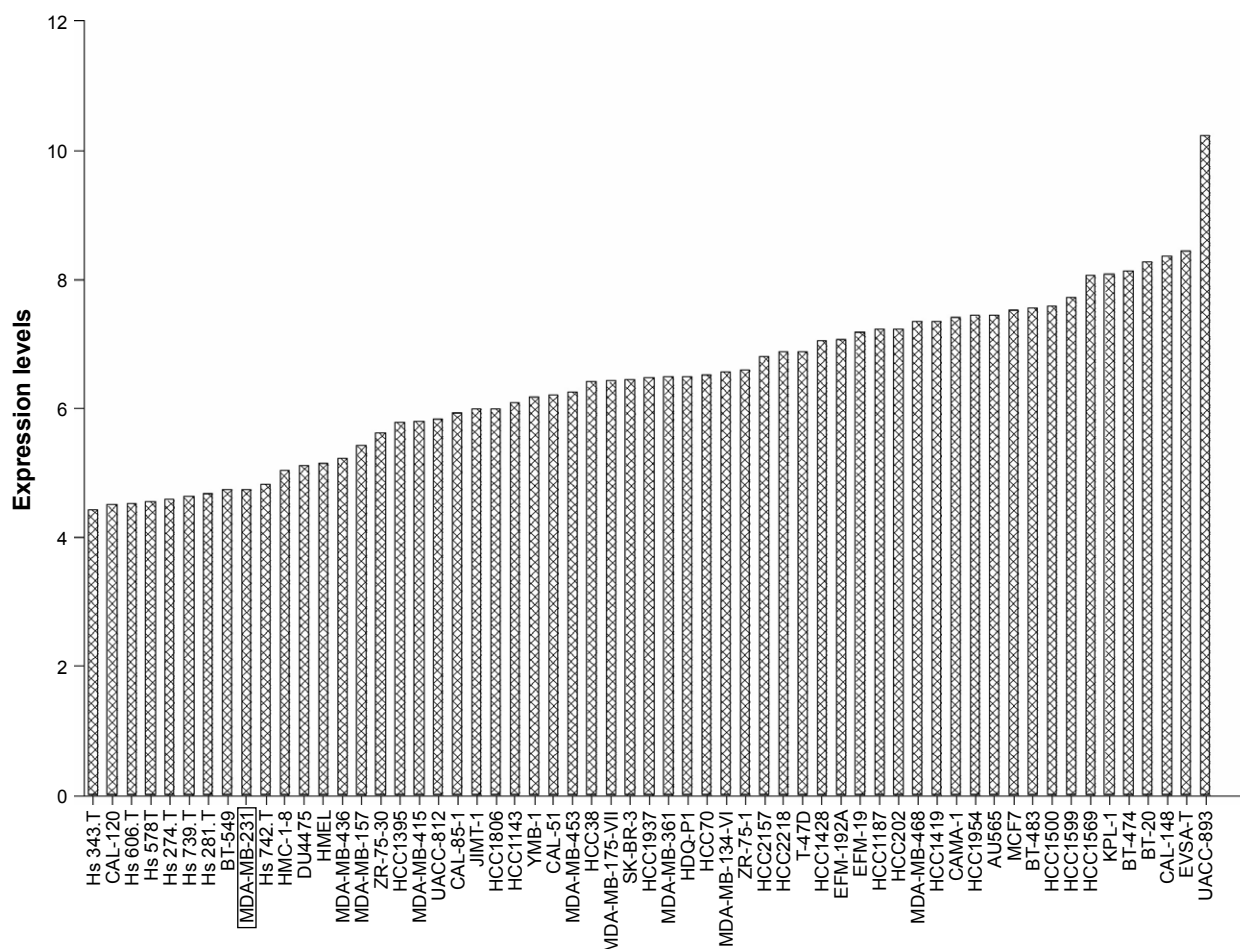
Figure S1 AIF1L expression levels in the breast cell of CCLE.
Note: Rectangle around MDA-MB-231 shows indicates AIF1L expression level was lower in MDA-MB-231 cell.
Abbreviation: CCLE, Cancer Cell Line Encyclopedia.